

---

## The Low-Resolution Structure of Human Muscle Aldolase [and Discussion]

J. R. Millar, P. J. Shaw, D. K. Stammers, H. C. Watson and J. D. G. Smit

*Phil. Trans. R. Soc. Lond. B* 1981 **293**, 209-214

doi: 10.1098/rstb.1981.0074

---

### Email alerting service

Receive free email alerts when new articles cite this article - sign up in the box at the top right-hand corner of the article or click [here](#)

---

To subscribe to *Phil. Trans. R. Soc. Lond. B* go to: <http://rstb.royalsocietypublishing.org/subscriptions>

---

## The low-resolution structure of human muscle aldolase

BY J. R. MILLAR, P. J. SHAW,<sup>†</sup> D. K. STAMMERS<sup>‡</sup> AND H. C. WATSON*Department of Biochemistry, University of Bristol, Bristol BS8 1TD, U.K.*

The three-dimensional structure of human muscle aldolase has been solved at 5 Å resolution with the use of two isomorphous heavy atom derivatives. The enzyme's four subunits are arranged about three mutually perpendicular intersecting twofold axes to form a compact spherical molecule. The subunit boundaries are clearly defined but a possible domain structure is not apparent in this preliminary electron density map.

## INTRODUCTION

Fructose-1,6-bisphosphate (FBP) aldolase (EC 4.1.2.13) is the glycolytic enzyme that cleaves a 6 (or 7) carbon chain to give a dihydroxyacetone phosphate (DHAP) and an aldehyde phosphate. The enzyme is a tetramer with a relative molecular mass of approximately 160 000, and has been widely studied as the classical example of an enzyme that forms a Schiff's base intermediate with one of its substrates (for review see Horecker *et al.* 1972). Crystals of the enzyme have previously been obtained from various muscle tissues (see, for example, Eagles *et al.* 1969) but, unlike those obtained for the trimeric 2-keto-3-deoxy-6-phosphogluconic aldolase (see Marvridis & Tulinsky 1976), they have proved unsuitable for detailed X-ray structural analysis. We report here the crystallization and preliminary X-ray structure studies with the aldolase extracted from human muscle tissue.

## CRYSTALLIZATION AND DATA COLLECTION

FBP aldolase was isolated from human muscle by using the affinity elution technique described by Scopes (1977) and crystallized from ammonium sulphate solution (440 g/l), buffered at pH 6.0 and stored at 4 °C. The hexagonal bipyramidal crystals shown in figure 1*a* grow over a period of about 1 month and, in our hands, have proved relatively stable to copper K $\alpha$  radiation. X-ray photographs show that in this crystal form there are three molecules in each unit cell ( $a = b = 96.5$  Å;  $c = 166.9$  Å;  $\alpha = 120^\circ$ ) and that the space group is either P6<sub>2</sub>22 or P6<sub>4</sub>22. These crystals are therefore essentially identical to the X-ray sensitive form obtained from rabbit muscle by Heidner *et al.* (1971), in which the asymmetric unit contains only one of the enzyme molecule's four subunits. By taking advantage of the stability to X-rays and the hexagonal symmetry of the human muscle crystals, it is possible to collect complete data sets from each specimen mounted on the Arndt–Wonacott rotation camera. Data were collected for several possible heavy atom derivatives by soaking native crystals in the appropriate solutions. The resulting photographs (for example figure 1*b*) were processed in exactly the same manner as those obtained from native crystals, to minimize errors when comparing different data sets.

<sup>†</sup> Present address: John Innes Institute, Colney Lane, Norwich NR4 7UH, U.K.

<sup>‡</sup> Present address: Wellcome Research Laboratories, Langley Court, Beckenham, Kent BR3 3BS, U.K.

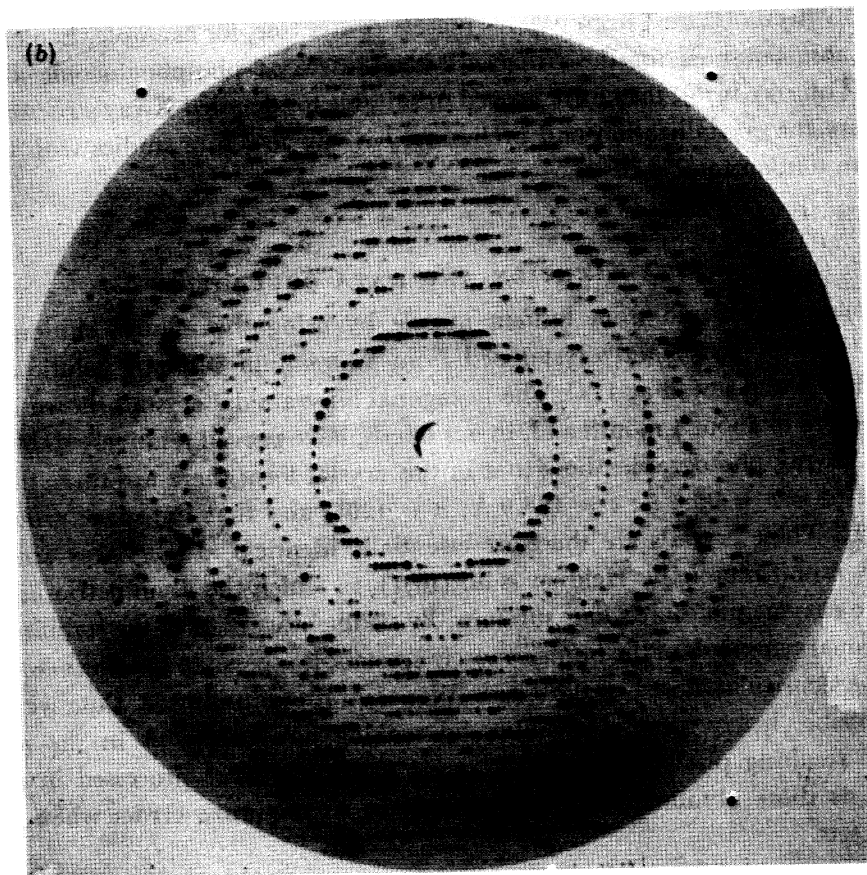
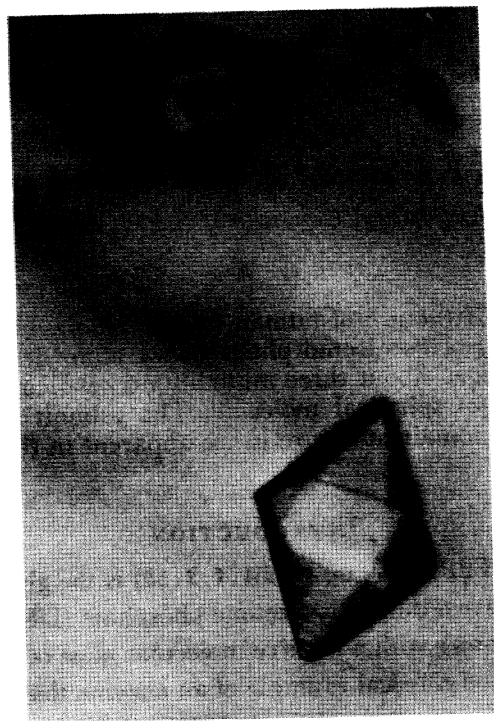


FIGURE 1. (a) Crystals of human muscle aldolase. The surface striations appear when the crystallization solution is allowed to reach room temperature. (b) Typical X-ray rotation ( $1.5^\circ$ ) photograph. The exposure was 6 h per film pack with sealed X-ray tube run at 40 kV and 40 mA; 12 film packs were obtained from each crystal.

## PHASE AND ELECTRON DENSITY CALCULATION

Difference Patterson maps calculated by using data collected from crystals with hexagonal space groups present special interpretative difficulties. Even for a fully substituted single-site derivative the expected peaks will be at or very near the error level. Following an extensive, semi-automated search, a reasonably satisfactory single-site solution was found for the *p*-CMB derivative in which approximately two-thirds of the expected vectors occurred on or near the Harker section shown in figure 2*a*. Phases calculated by using the single-site solution for the

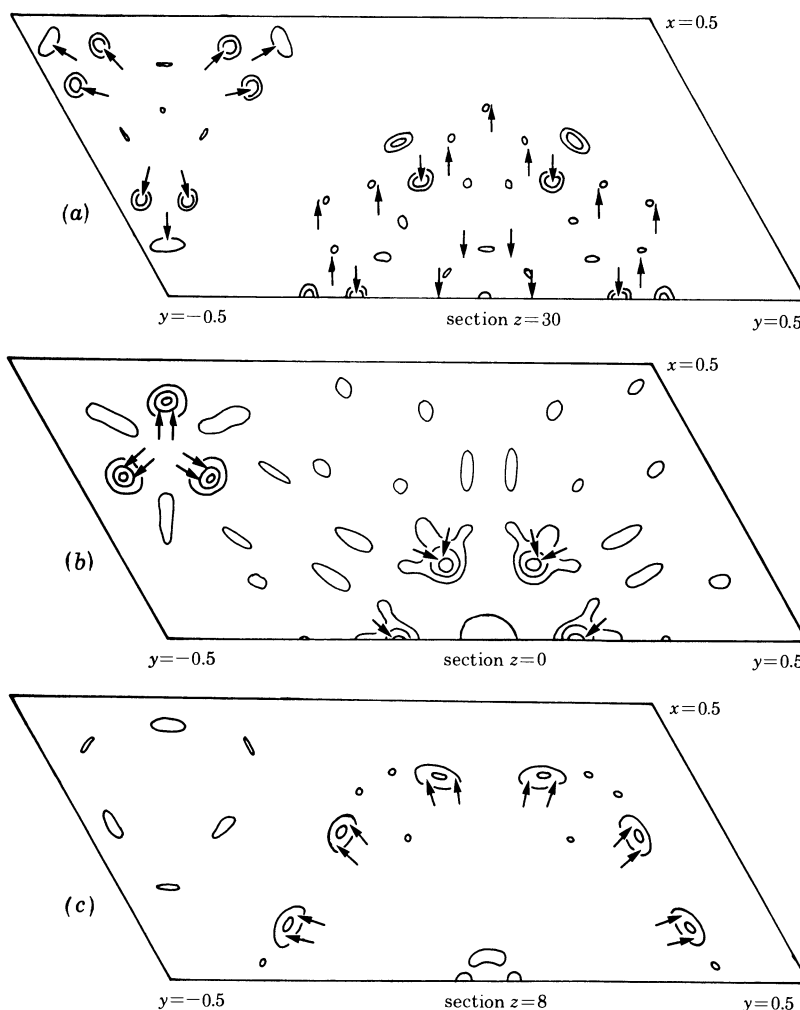


FIGURE 2. Selected sections from the two 5 Å resolution difference Patterson maps. Expected heavy atom vectors are indicated by arrows. The maps were calculated in 90 sections perpendicular to the sixfold axis. (a) Harker section for the *p*-CMB difference Patterson function. (b) Harker section for the  $\text{PtCl}_4$  difference Patterson function. Note that the two sets of self vectors group in pairs, producing double weight peaks. (c) The Patterson section showing the cross vector positions for the two-site  $\text{PtCl}_4$  derivative.

*p*-CMB derivative were used to calculate a difference Fourier map for the  $\text{PtCl}_4$  derivative. This map revealed two major platinum sites whose positions were verified by using the previously uninterpretable  $\text{PtCl}_4$  Patterson map shown in figure 2*b, c*. Phases derived from the two-site solution for the platinum derivative were also used to confirm the interpretation of the *p*-CMB Patterson difference map. This difference Fourier calculation indicated a second

TABLE 1. THE HEAVY ATOM OCCUPANCY AND POSITIONAL PARAMETERS

( $x$ ,  $y$  and  $z$  are fractional coordinates. The heavy atom temperature parameters were set to 15.0 and not refined.)

site	occupancy	$x$	$y$	$z$
PtCl <sub>4</sub> 1	1.0453	0.3567	0.6547	0.0693
2	0.9044	0.0011	0.4252	0.1623
<i>p</i> -CMB 1	0.9045	0.1754	0.6242	0.9954
2	0.4741	0.0751	0.8942	0.0739

TABLE 2. THE PHASE AND REFINEMENT PARAMETERS

( $|F|$  is the mean protein structure amplitude;  $R_c$  and  $R_k$  are the standard crystallographic and Kraut refinement indicators, respectively;  $f$  is the heavy atom structure amplitude and  $E$  is the lack of closure error. Reflexions with a lack of closure error greater than 5.0 or with a figure of merit less than 0.3 were not included in the phase refinement process. The average figure of merit for the 1484 reflexions included in the calculation of the 5 Å resolution electron density map was 0.762.)

derivative	$ F $	$R_c$	$R_k$	$f/E$
PtCl <sub>4</sub>	20.24	0.474	0.076	2.36
<i>p</i> -CMB	21.09	0.641	0.070	1.71

*p*-CMB binding site. Subsequent refinement of the heavy atom parameters (see table 1) suggested that the occupancy of the second *p*-CMB binding site was approximately half that of the major site. Details of the phase and refinement parameters are given in table 2.

A 'mini'-map corresponding to the 'best' Fourier synthesis (Blow & Crick 1959) at 5 Å resolution showed that the molecular boundary could be traced quite easily despite the close packing of adjacent molecules. The subunit boundaries were also delineated with little difficulty. The three intersecting twofold axes are generally devoid of electron density, and confirmation of the overall correctness of the structure comes from the fact that all the derivative binding sites are readily accessible from the surrounding solvent.

#### A LOW-RESOLUTION MODEL

A photograph of the balsa-wood model of the enzyme is shown in figure 3. The complete molecule is approximately spheroidal. The darker subunit shows that each monomer is ellipsoidal with an axial ratio of approximately 2:1. The subunit packing arrangement is such that the contact between pairs of monomers (front and back in figure 3) is more extensive than between dimers. In general, the subunit surface appears devoid of clefts or deep depressions. An analysis of the amino acid sequence data for the rabbit enzyme has led to the prediction that the subunit would contain an NAD-type binding domain (Stellwagen 1976). Although such a structural feature could well exist in our preliminary low-resolution model, it is not immediately apparent.

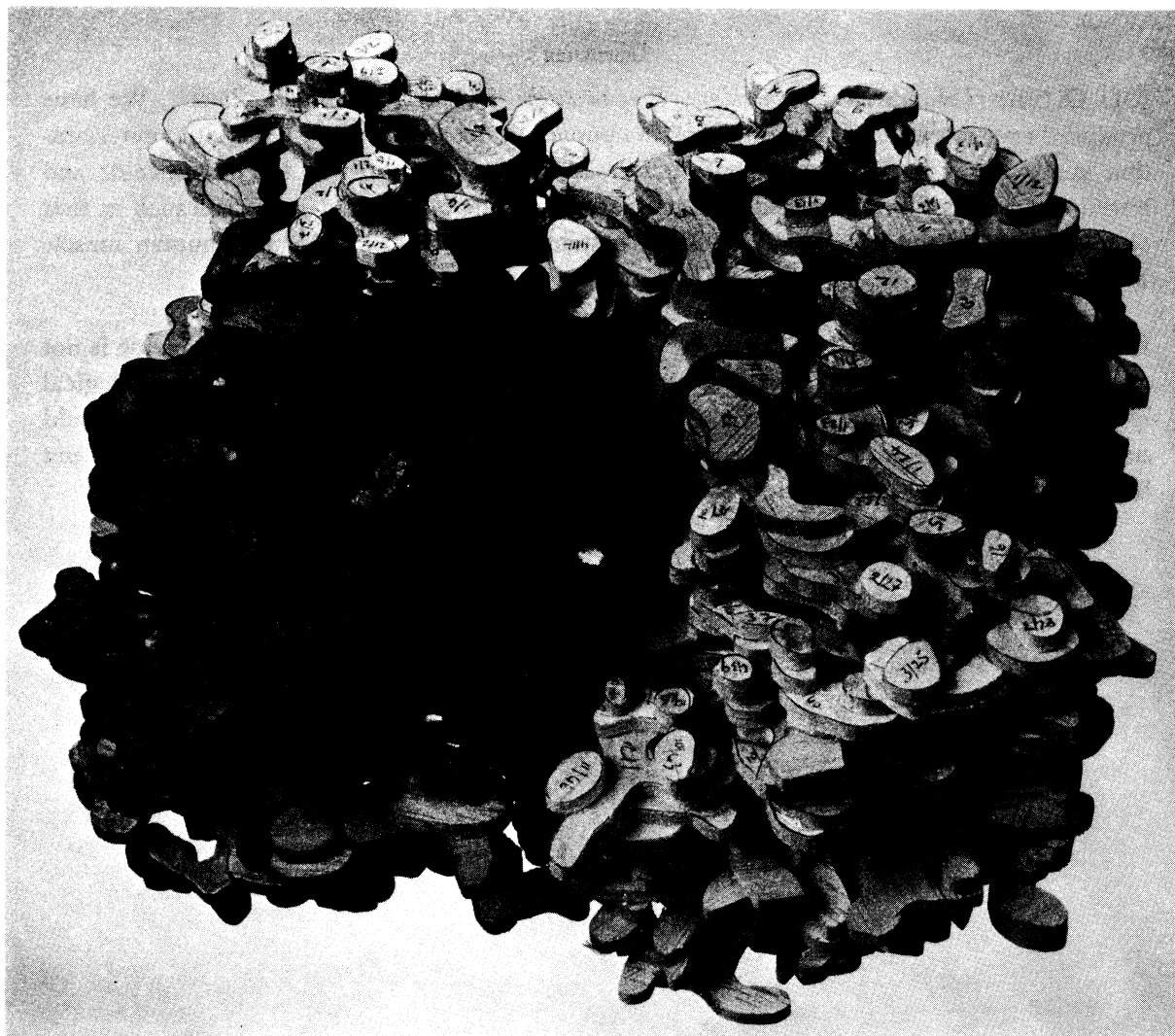


FIGURE 3. A photograph of a balsa-wood model of the enzyme. One of the four aldolase subunits has been coloured. The heavy atom binding positions are marked with small plastic beads. One of the  $\text{PtCl}_4$  sites can be seen at the extreme left centre of the darker subunit. A  $p$ -CMB site appears on the darker subunit towards the top of the central inter-subunit cleft.

#### REFERENCES (Millar *et al.*)

- Blow, D. M. & Crick, F. H. C. 1959 Treatment of errors in the isomorphous replacement method. *Acta crystallogr.* **12**, 794–802.
- Eagles, P. A. M., Johnson, L. N., Joynson, M. A., McMurray, C. H. & Gutfreund, H. 1969 Subunit structure of aldolase: chemical and crystallographic evidence. *J. molec. Biol.* **45**, 533–544.
- Heidner, E. G., Weber, B. H. & Eisenberg, D. 1971 Subunit structure of aldolase. *Science, N.Y.* **171**, 677–679.
- Horecker, B. L., Tsolas, O. & Lai, C. Y. 1972 Aldolases. In *The enzymes* (ed. P. Boyer), vol. 7, pp. 213–258. New York: Academic Press.
- Mavridis, I. M. & Tulinsky, A. 1976 The folding and quaternary structure of trimeric 2-keto-3-deoxy-6-phosphogluconic aldolase at 3.5 Å resolution. *Biochemistry, Wash.* **15**, 4410–4417.
- Scopes, R. K. 1977 Purification of glycolytic enzymes by using affinity-elution chromatography. *Biochem. J.* **161**, 253–263.
- Stellwagen, E. 1976 Predicted structure for aldolase. *J. molec. Biol.* **106**, 903–911.

*Discussion*

J. D. G. SMIT (*Laboratorium für Biochimie, Eidgenössische Technische Hochschule, Zürich*). We have produced crystals of aldolase (from *Drosophila* pupae) that are reasonably resistant to deterioration in the X-ray beam. We attribute this resistance at least partly to the low cysteine and histidine content of *Drosophila* aldolase compared with the other class I aldolases such as that obtained from rabbit muscle. What is the cysteine and histidine content of human muscle aldolase?

H. C. WATSON. Unfortunately the amino acid sequence for the human muscle enzyme is not available. Several examples exist of sequences of the same enzyme from different biological sources. These data indicate that the glycolytic enzymes are highly conserved and would suggest that the amino acid sequence (and composition) of human muscle aldolase will not be very different from that of the rabbit.

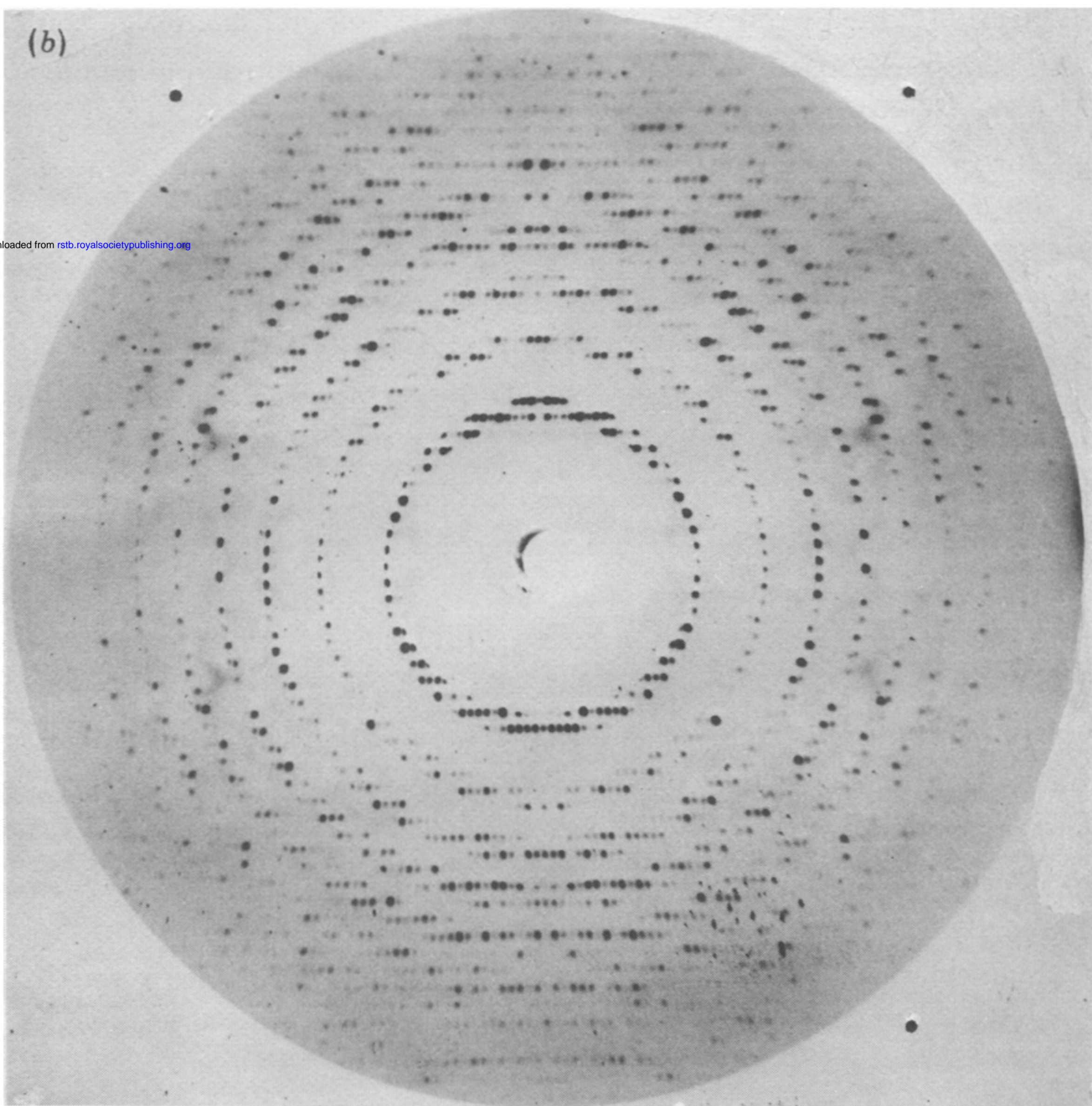
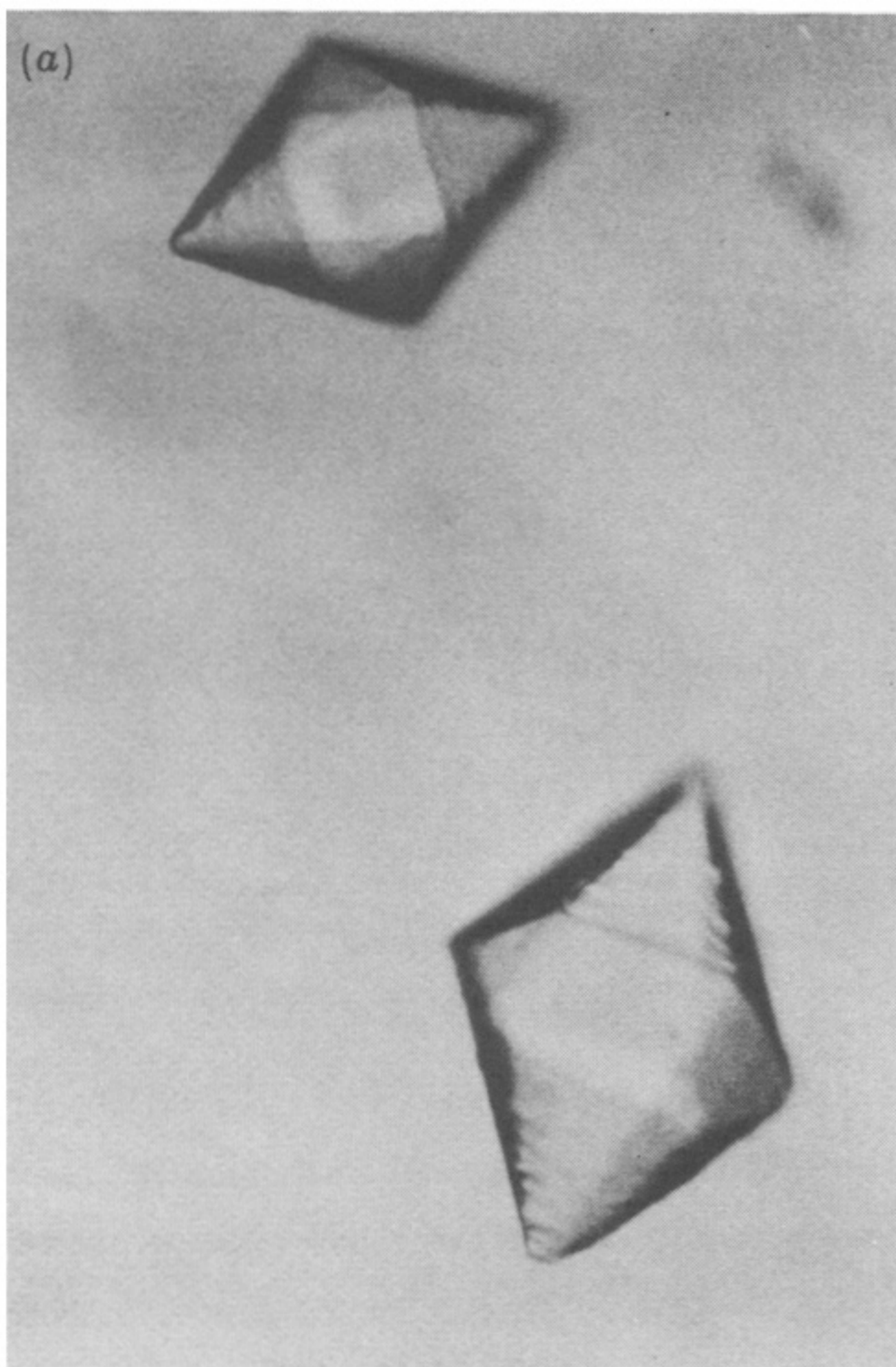


FIGURE 1. (a) Crystals of human muscle aldolase. The surface striations appear when the crystallization solution is allowed to reach room temperature. (b) Typical X-ray rotation ( $1.5^\circ$ ) photograph. The exposure was 6 h per film pack with sealed X-ray tube run at 40 kV and 40 mA; 12 film packs were obtained from each crystal.



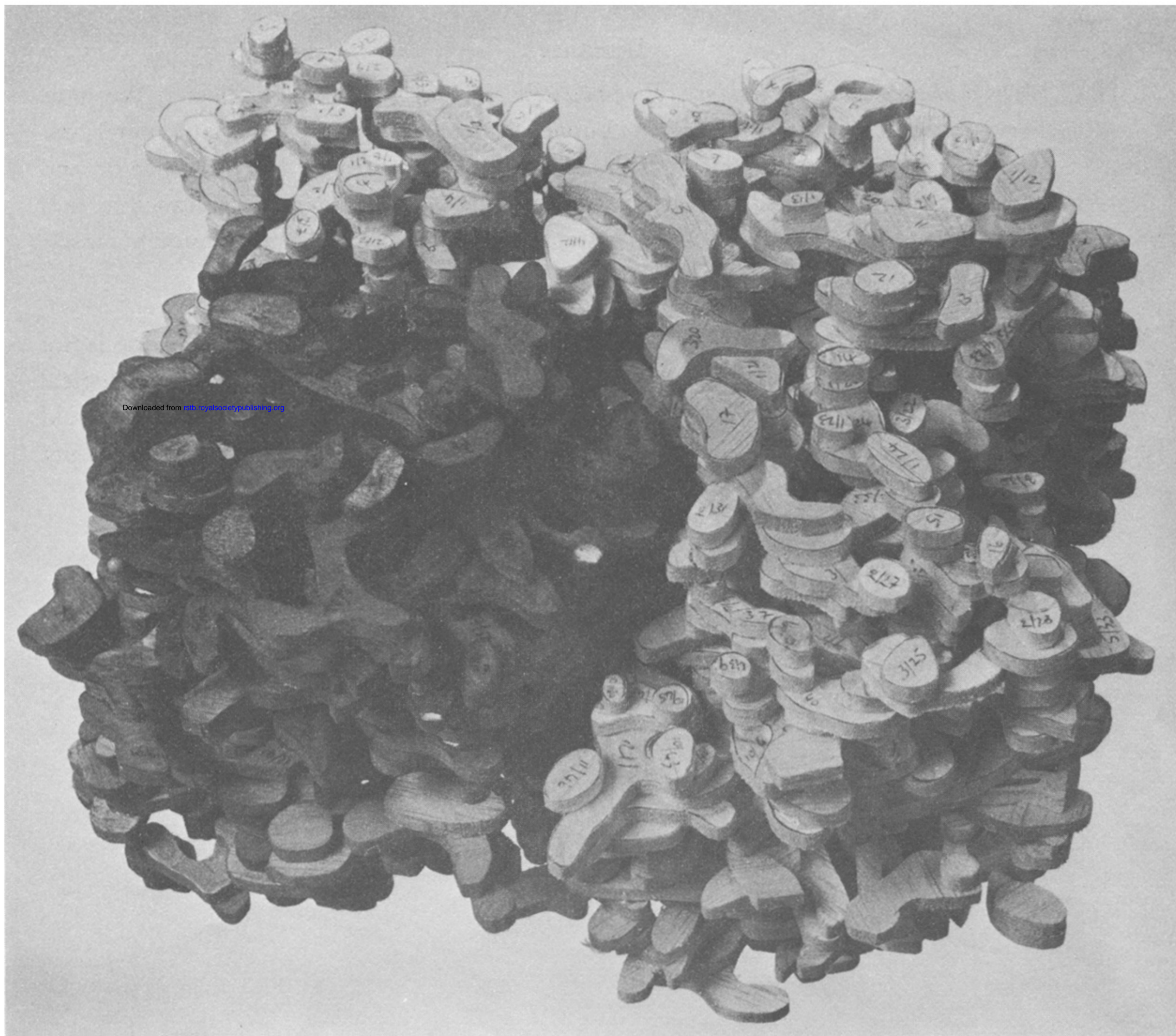


FIGURE 3. A photograph of a balsa-wood model of the enzyme. One of the four aldolase subunits has been coloured. The heavy atom binding positions are marked with small plastic beads. One of the  $\text{PtCl}_4$  sites can be seen at the extreme left centre of the darker subunit. A *p*-CMB site appears on the darker subunit towards the top of the central inter-subunit cleft.